Eleventh International Conference on Computational Fluid Dynamics (ICCFD11), Maui, HI, USA July 11-15, 2022 **ICCFD11-2022-0202**

Atmospheric Boundary Layer simulations with a LES model nested in a regional atmospheric simulation.

M. Bove*, A. Vignolo*, M. Mendina*, G. Usera* and G. Cazes*
Corresponding author: mbove@fing.edu.uy

* Facultad de Ingeniería, Universidad de la República

Abstract:
Many science and engineering problems involve accurate modelling of the Planetary Boundary Layer (PBL). Doing so requires simultaneous representation of a wide range of scales, from the synoptic and mesoscale to the three-dimensional boundary layer turbulence. This is still an open problem, although many efforts have been made in order to attain realistic atmospheric multi-scale simulations.
In this paper an offline unidirectional coupling strategy with successive finer nested grids is implemented to incorporate realistic meteorological information from the Weather Research and Forecasting (WRF) mesoscale model into an in-house Large Eddy Simulation (LES) model, called caffa3d.
This tool is tested for a case day with a Convective Boundary Layer (CBL) in a region of interest over real terrain. Preliminar results show a good assimilation of WRF fields into caffa3d's finer grids. It is shown that the fetches considered are enough for turbulent motion to develop, although larger domains are needed for a full stabilization of turbulent statistics.

Keywords: CFD, LES, WRF, coupling, nesting, mesoscale, microscale, PBL.

1 Introduction

Many science and engineering problems, such as wind energy production, flow over complex terrain, pollutants transport and meteorological prediction of certain clouds, depend on the Planetary Boundary Layer (PBL) [1], which is the portion of the troposphere that is directly influenced by the Earth's surface [2]. Accurate modelling of PBL phenomena requires simultaneous representation of a wide range of scales, from the synoptic and mesoscale to the three-dimensional boundary layer turbulence [3]. Numerical Weather Prediction (NWP) models are extensively used for mesoscale simulations, with domain dimensions ranging from a few hundreds meters to a thousand kilometers. However, the relatively coarse resolution of these models cannot capture the microscale dynamics of the PBL [4].

An alternative to NWP models is the Large Eddy Simulation (LES) approach, which can represent the microscale variability of the low atmosphere. The first three-dimensional, time-dependent numerical simulations of turbulent flow with spatial and temporal resolution adequate to resolve the dynamics and evolution of the energy-containing eddies were conducted in 1972 by Deardoff [5, 6]. Since then, LES has been extensively used to reproduce a variety of PBL regimes and to better investigate some atmospheric problems, as it explicitly resolves the most energetic turbulent scales, thus enabling to recreate the microscale dynamics of the lower atmosphere. Nevertheless, to resolve all the relevant scales involved in atmospheric flows using LES, a very large domain with fine resolution is needed, which is computational prohibitive. Besides, in order to incorporate realistic meteorological information a NWP model is needed. This problem can be alleviated by bridging mesoscales and microscales through grid-nesting techniques, where a boundary condition obtained from coarser grids is prescribed to the finer ones [1, 3, 7, 8, 9].

In recent years efforts have been made to tackle dynamical downscaling of NWP models beyond their usual mesoscale scope. Most attempts have utilized the Weather Research and Forecasting (WRF) [10] model alongside its nesting and LES modelling capabilities [11, 12, 13, 14, 15]. However, it has been shown that PBL simulations can be conducted by combining mesoscale models, such as WRF, with other LES simulation software. This can be done via an offline coupling approach, were fields are extracted from the mesoscale NWP model solution and imposed as boundary conditions to the LES solver [3, 16, 17].

Coupling NWP and LES models is a challenging endeavor. One of its main problems is that turbulence does not instantaneously develop within the LES domain. This happens because WRF and most of the NWP models use a Reynolds Averaged Navier Stokes (RANS) [10] approach, which provides time-averaged fields and does not resolve any turbulent scale explicitly. Therefore, the boundary conditions obtained for the nested LES domain are smooth (i.e. do not contain any turbulence) [3, 7, 18, 19, 20]. As a consequence, long fetches are required for turbulence to emerge. This generates an under-developed transitional state which affects turbulence related magnitudes and modifies the structure of the simulated PBL. This is particularly relevant in the Convective Boundary Layer (CBL), which needs turbulent mixing to develop its whole plethora of phenomena [2, 3].

Another challenge that requires careful attention in multi-scale simulations is the so called *terra incognita* or *gray zone* [21], which refers to the situation where the grid resolution (Δ) is of the same order of the dominant length scale (l) of the flow field. For instance, in a daytime CBL the flow length scale is given by the order of its largest eddies, which are in the order of the planetary boundary layer (PBL) depth ($l \sim 1\,\mathrm{km}$). To avoid falling in the *terra incognita*, Δ should be much smaller than the PBL depth [22]. Nonetheless, when dealing with atmospheric multi-scale simulations this is seldom the case.

A key aspect for nesting NWP and LES simulations is determining at which spatial resolution one should switch from the mesoscale approach, in which the PBL is unidimensional and fully parametrized, to the LES approach, where larges eddies are resolved and the flow is tridimensional. Several studies have shown that mesoscale schemes result in partially resolved convective structures that are a numerical artifact [3, 23, 24]. It has been recently shown [1] that if these structures are prescribed as a boundary condition to the LES domain, the diameter of the convective cells resolved by the LES domain decreases. Furthermore, and most importantly, the development of turbulence within the LES domain is delayed. Therefore, longer fetches are required. Still, given a long enough fetch, turbulence will finally devolop and most PBL related magnitudes will be accurately resolved, thus encouraging the implementation of nesting strategies.

In this work, we present an offline unidirectional coupling technique from the WRF NWP model to the in-house caffa3d LES model [25, 26, 27]. Successively finer nested grids are used to improve the caffa3d's ability to model the PBL turbulent scales. This technique is used to model the convective boundary layer (CBL) in a case day in a region of interest over real terrain.

The article is organized as follows: Section 2 briefly presents the numerical models used, Section 3 describes the coupling strategy together with the case study used to test it. In Section 4 an account of the LES simulation setup and case setting is done, Section 5 shows the obtained results and discuss it. In Section 6 a summary of the work is done and some conclusions are drawn. Finally, in Section 7 future work is discussed.

2 Numerical models

2.1 WRF

WRF, the mesoscale model used, is an atmospheric modelling system designed for both research and numerical weather prediction. It is open-source and has been adopted for research at universities and governmental laboratories, for operational forecasting by governmental and private entities, and for industrial applications.

Advanced Research WRF (ARW) is a particular configuration of WRF. It solves fully-compressible, non-hydrostatic Eulerian equations. Additionally, a run-time hydrostatic option is available [10].

2.2 caffa3d

For the LES simulations an open-source, finite volume CFD solver called caffa3d is used. This solver has second order accuracy in space and time, and is used to simulate three-dimensional incompressible flows in block structured curvilinear grids.

The domain is divided in unstructured blocks of structured grids. The same block structure is used for parallelization through MPI [25] by domain decomposition. The mathematical model comprises the mass balance equation (1) and momentum balance equation (2) for a viscous incompressible fluid, together with generic passive scalar transport equation (3) for scalar field ϕ with diffusion coefficient Γ. The balance equations are written for a region Ω, limited by a closed surface S, with outward pointing normal $\hat{n}_s$

$$\int_S (\vec{v} \cdot \hat{n}_s)\, dS = 0 \tag{1}$$

$$\int_\Omega \rho \frac{\partial u}{\partial t} d\Omega + \int_S \rho u\, (\vec{v} \cdot \hat{n}_s)\, dS = \int_\Omega \rho\beta(T - T_{ref})\vec{g} \cdot \hat{e}_1\, d\Omega + \int_S -p\hat{n}_s \cdot \hat{e}_1\, dS + \int_S (2\mu D \cdot \hat{n}_s) \cdot \hat{e}_1\, dS \tag{2}$$

$$\int_\Omega \rho \frac{\partial \phi}{\partial t}\, d\Omega + \int_S \rho\phi\, (\vec{v} \cdot \hat{n}_s)\, dS = \int_S \Gamma\, (\nabla\phi \cdot \hat{n}_s)\, dS \tag{3}$$

where $\vec{v} = (u, v, w)$ is the velocity, ρ is the density, β is the thermal expansion factor, T is the temperature and T_{ref} a reference temperature, $\vec{g}$ is the gravity, p is the pressure, μ is the dynamic viscosity of the fluid and D is the strain tensor.

The generic transport equation (3) for passive scalars can be used to implement other physical models like heat transport and turbulence models, especially used in these simulations. The use of equations in their global balance form, together with the finite volume method, as opposed to the differential form, favors enforcing conservation properties for fundamental magnitudes as mass and momentum into the solving procedure [25, 26, 27].

To handle correctly the linearization and subsequent coupling of linear systems for each equation in the mathematical model, an outer-inner iteration scheme for each time step is used, as shown in Fig. 1. Regarding the subgrid modelling the standard Smagorinsky model with a coefficient of 1.6 was used. [28].

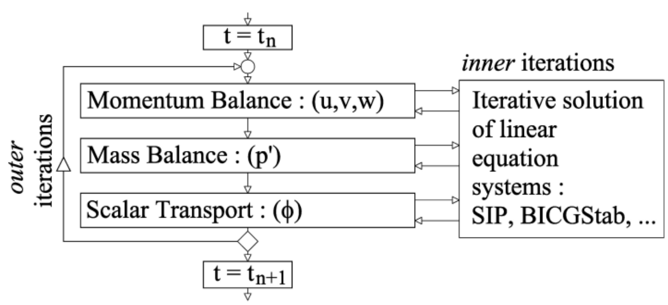

Figure 1: Iteration scheme for one time step. Extracted from [25].

The nested overlapping grids module of caffa3d [29] was used in order to nest grids of different resolutions and sizes. This module is based on the work of Hadzic [30] where overlapping grids of different resolutions are generated and the information at every time step is interpolated. A scheme with active, passive and interpolation cells is created to manage this procedure.

2.2.1 Adiabatic expansions and compressions

A modification to caffa3d flow solver source code was done in order to model the adiabatic expansions and compressions that occur in a compressible flow exposed to changes in temperature, like air in the atmosphere.

In a CBL, vertical vortices associated with the ascent of hot air and descent of cold air are developed. The air parcels in these vortices experiments adiabatic expansions and compressions when ascending and descending, respectively. This cooling and heating increases and decreases the density of air parcels, which stabilizes the effect of the buoyancy and limits the height of the eddies. [2]

As caffa3d is designed to simulate incompressible flows, it cannot recreate the previously described physical phenomenon without some modification on its source code. That is because the energy balance equation does not contain a term associated with compression mechanical work. It is therefore proposed, to incorporate the thermal effects of compression mechanical work in a explicit way into caffa3d source code. Starting off with the First Law of Thermodynamics:

$$c_p \frac{dT}{dt} = \dot{q} + \nu \frac{dP}{dt} \tag{4}$$

where c_p is the specific heat capacity at constant pressure, T is the temperature, $\dot{q}$ the thermal power supplied to the fluid and P is the pressure. The term on the left represents the total differential of the sensible enthalpy, the first term on the right accounts for the thermal power supplied to the fluid, and the second one is the compression mechanical work. This last term is the one that caffa3d lacks and will be explicitly modelled.

Approximating the pressure field by an hydostatic distribution and differentiating in time, the following expression is obtained:

$$\frac{dP}{dt} \approx -\rho g U_z \tag{5}$$

where U_z is the vertical component of the velocity field.

Hence, the main thermal effects associated with adiabatic expansions and compressions due to the ascent or descent of air parcels can be represented in caffa3d by adding this term to the right side of Equation 3.

This implementation was tested in the coupling presented in this work. Results show that eddies are constrained in height as appreciated in Fig. 2.

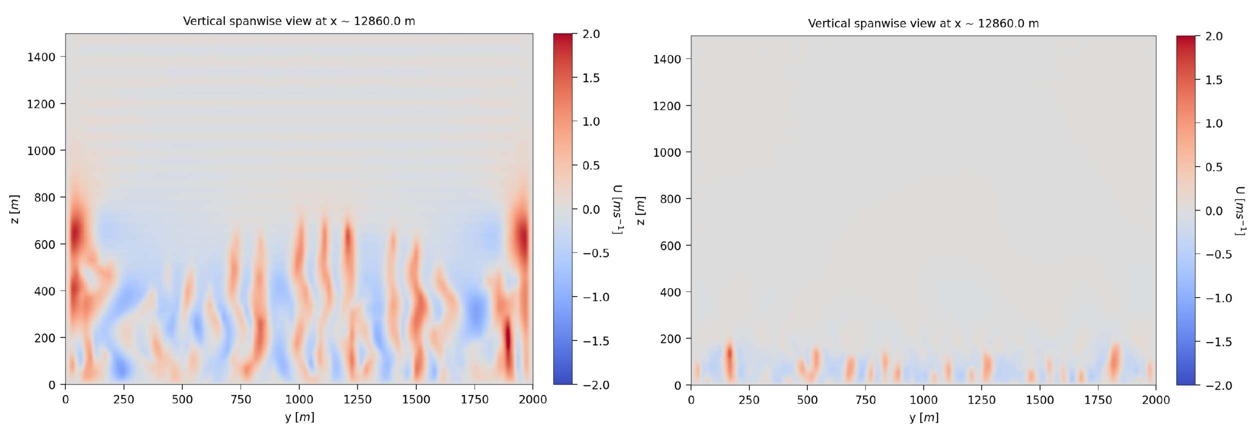

(a) (b)

Figure 2: Spanwise slices of the vertical velocity component at a position 12.86 km from the inflow for a LES simulation with uniform velocity and temperature profiles (a) without the term that takes adiabatic expansion and compressions into account and (b) with the term.

3 Coupling methodology and case study

An offline unidirectional coupling between the mesoscale WRF model and the in-house caffa3d LES model was implemented. The strategy consists in processing WRF simulations fields and adapting them to be prescribed as initial and boundary conditions for the LES model. The velocity, temperature and surface heat flux fields are used. The pressure field is not imposed, as that would overdeterminate of the discretized equations system.

WRF works with an Arakawa C grid system, whereas caffa3d uses Arakawa A grid, thus a transformation of the relevant fields was performed [31].

The surface layer was modeled using the Monin-Obukhov similarity theory [32], namely, the velocity was extrapolated to the cell centers near the ground using similarity theory. The other fields were extrapolated with a second order polynomial.

Then, a new caffa3d module was implemented to read these fields on execution time and prescribe them as initial and inflow boundary condition on each time step. This can be done dynamically, namely, WRF fields from different times can be prescribed on execution to caffa3d in order to dynamically update the boundary conditions. Although this is already implemented, in this work the stationary situation is presented.

3.1 Topography and geographic location

In the context of the NEFELE project (see Section 8) a region of interest, near Salto city in the department of Salto, Uruguay was taken to conduct the WRF simulations and test the coupling of the two models. In Fig. 3 the geographic location of the study region within South America and its topography can be appreciated.

In order to realistically simulate this geographical location, the topography was included into the LES domain. This has the the advantage of increasing the mechanical generation of turbulence which may improve the modelling of the PBL, specially of the surface layer [19].

Although the WRF mesoscale model includes a terrain-following vertical coordinate that contemplates the topography of the region, this is too coarse for the refined LES domains. Therefore the need for having a finer topography. This high resolution topography is obtained from satellite information provided by the Advanced Spaceborne Thermal Emission and Reflection Radiometer Global Digital Elevation Model Version 3 (ASTER-GDEM 003) [33]. This information is processed using the software library NetCDF [34] and adapted to the format required by the LES model caffa3d, namely, to transform the high resolution topography given in geographical (spherical) coordinates to Cartesian coordinates and bilinearly interpolate it to the resolution of the LES domain.

Fig. 4 shows a comparison between the WRF and the interpolated ASTER-GDEM topographies. Notice that ASTER-GDEM topography correctly represents the flooded area of the Salto Grande dam's reservoir, whereas WRF topography does not. Besides, there is a discontinuity in the ASTER-GDEM topography that corresponds to the dam and the dam's reservoir. Due to being near a river the region's terrain is mostly flat with some low hills at the south-east direction. Thus, it is expected that the shear turbulence does not contribute too much to the total turbulence budget. [2]

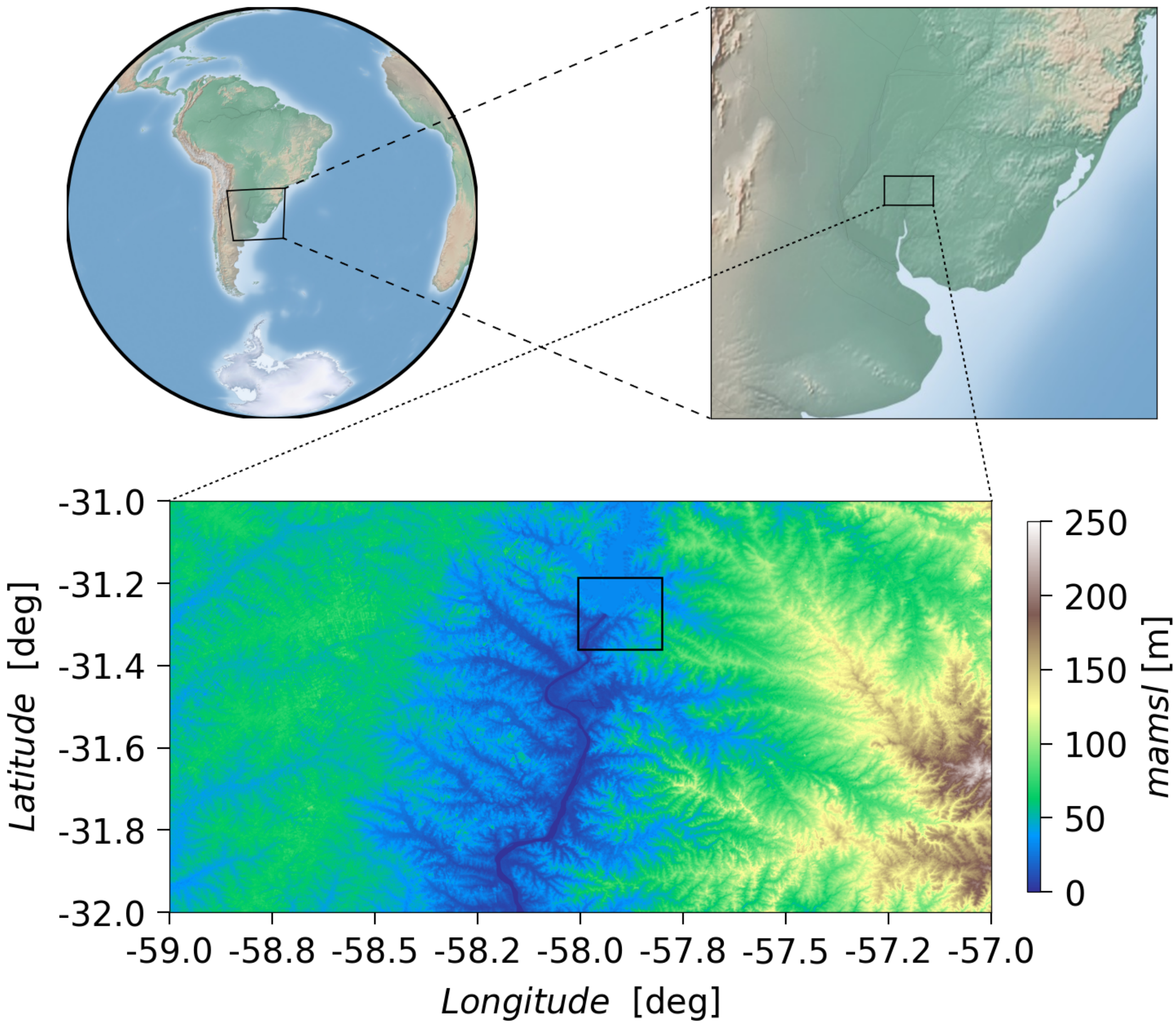

Figure 3: Location of the region of study within the world and South America. At the bottom, DEM topography from ASTER-GDEM [33] of Uruguay River basin, the rectangle delimits the WRF simulation domain.

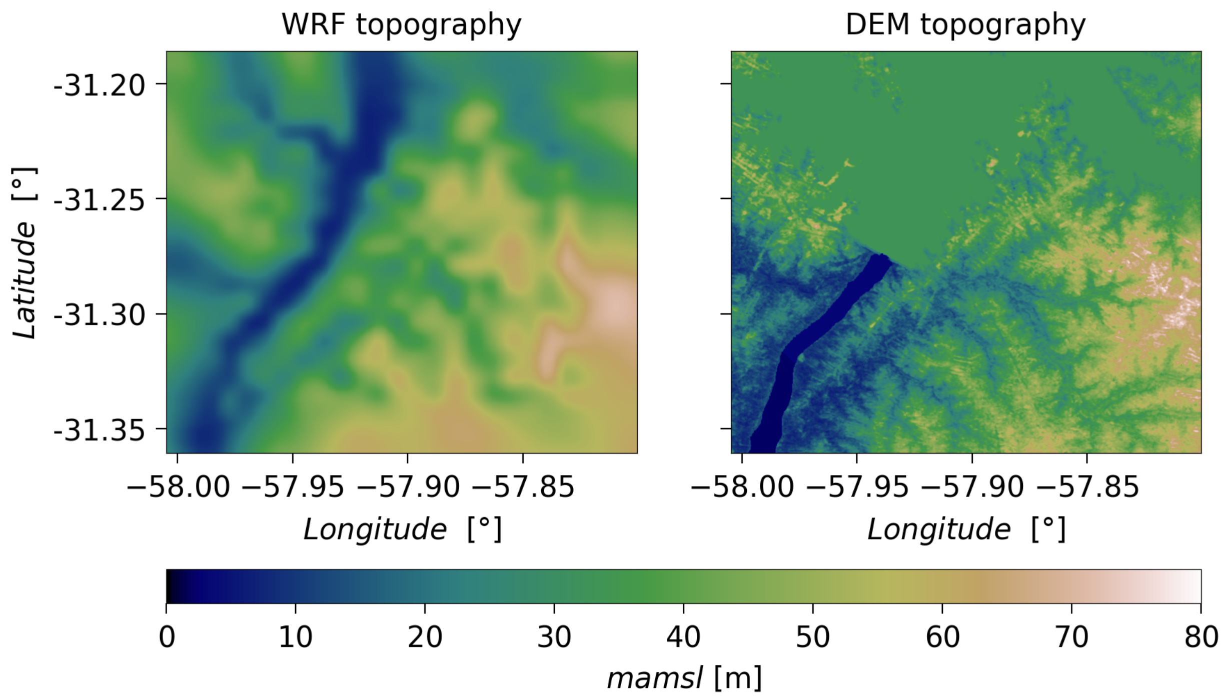

Figure 4: Topography of the study region (WRF simulated area) alongside Uruguay River on Salto, Uruguay. On the left, WRF default topography, and on the right, ASTER-GDEM topography of the same region.

3.2 WRF simulation

The region indicated with a rectangle at the bottom subplot of Fig. 3 was simulated in WRF with $64 \times 64 \times 99$ cells, with a horizontal resolution of 312 m, a vertical resolution of 30 m, and up to a height of 9450 m. In these simulations, the Yonsei University (YSU) PBL scheme [35, 36] was used. This is a first-order non-local scheme, with a countergradient term and an explicit entrainment term in the turbulence flux equation which has been widely used in meteorological simulations [37].

The morning of the 23/11/2018 was chosen to be simulated for three hours: 10, 11 and 12 GMT−3, uruguayan time. This time and date were selected due to the convective PBL and capping inversion that this morning presents at the center of the domain (see Fig. 5a). The vertical profile of potential temperature and the dry static energy, which is closely related to the potential temperature, depend on both the strength of the prescribed heat flux, and whether or not the PBL is well mixed [1].

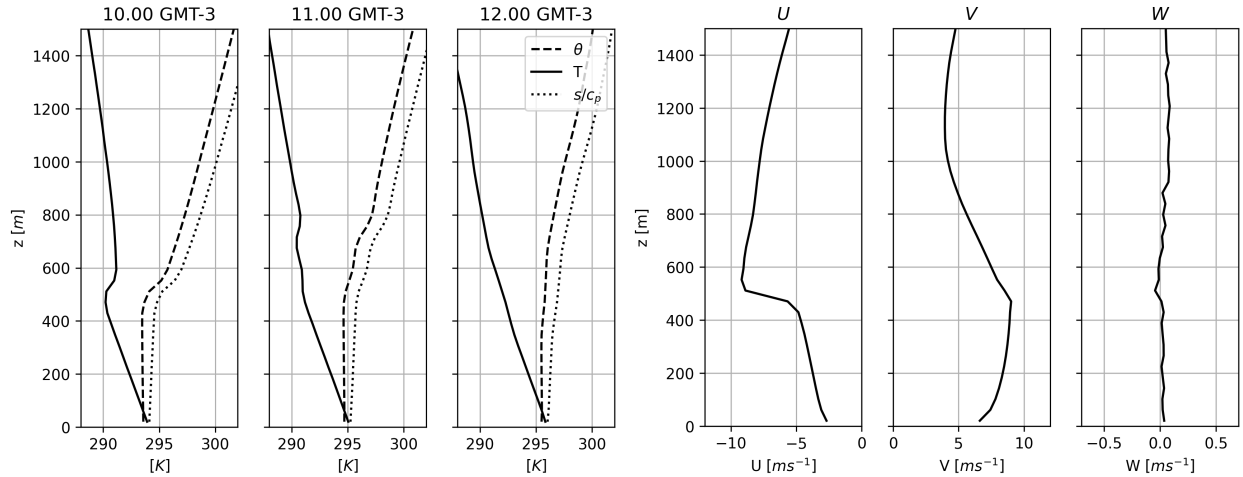

(a) (b)

Figure 5: (a) Absolute temperature, potential temperature and dry static energy divided by specific heat profiles of the WRF simulation. This morning was selected due to its clear capping inversion at 10 GMT−3. (b) WRF velocity profiles at 10 GMT-3, uruguayan time.

This domain has a non-uniform *TKE* field as depicted in Fig. 6, with lower values above the Salto Grande water reservoir, as it is a flat surface and does not liberates much heat to the surrounding air due to the large heat capacity of water (see Fig 7). The *TKE* profile (middle subplot of Fig. 6) follows the typical behaviour of a morning PBL, that is, it collapses to zero above the capping inversion that is shown at the right of Fig. 6.

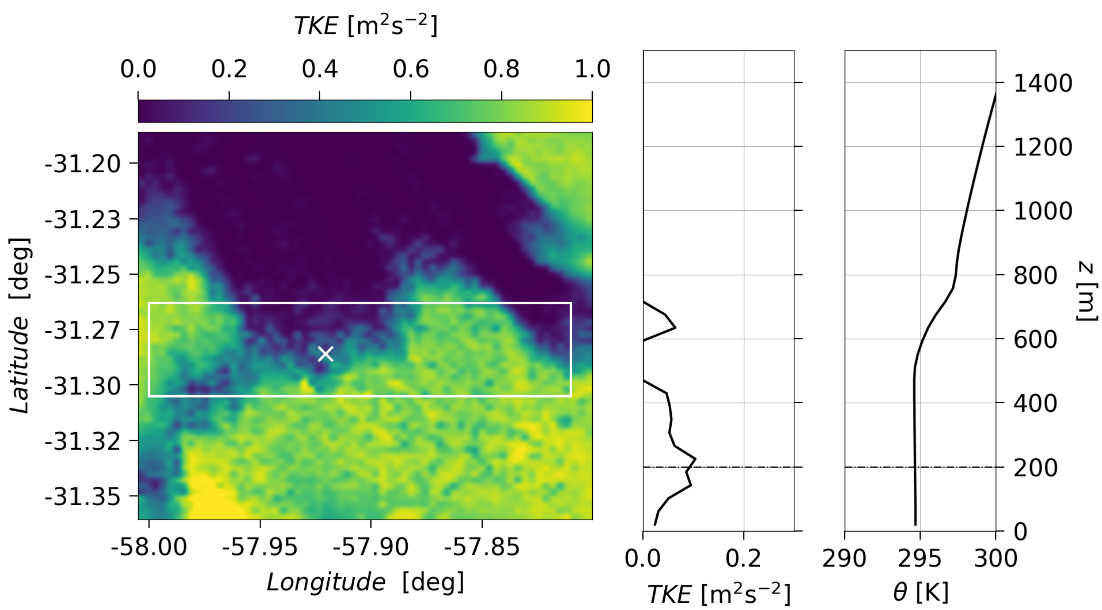

Figure 6: At the left, WRF simulation non-resolved *TKE* field at $z \sim 200\,\mathrm{m}$. LES outermost domain perimeter depicted in white. A white cross indicates the position for the *TKE* and θ profiles that are shown in the middle and the right subplots respectively.

As the PBL height and all its characteristics are determined by its interaction with the ground, it is essential to correctly assimilate the surface heat fluxes that naturally occur due to solar heating (or radiation cooling at night or when stratocumulus are present [38]). Therefore, the WRF surface heat flux was prescribed at the surface of the LES domain. Several studies have shown that this flux accelerates development of turbulence in the LES simulations [19].

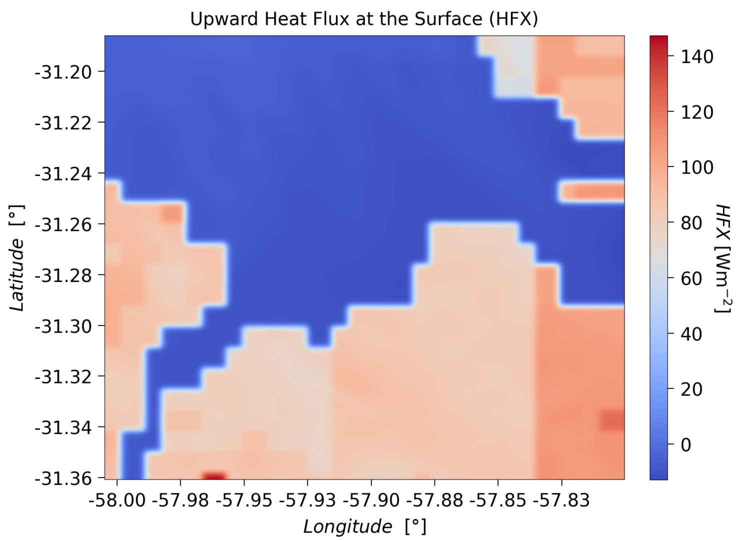

Figure 7: Upward Heat Flux at the Surface (HFX) of the WRF simulation.

4 Simulation setup

In this section the LES simulation setup is described. As mentioned in Section 3, the WRF velocity, temperature and surface heat flux fields are prescribed at the inflow boundary condition to the LES domain.

A nesting strategy with successively finer LES domains is implemented. The outermost LES domain is the one which receives the inflow conditions of the WRF simulation. Fig. 8a shows the disposition of this outermost LES domain with respect to the whole WRF domain and the ASTER-GDEM topography of the region.

The prevailing wind direction of the WRF simulation was rotated in order to align the flow with the x axis. This simplifies the prescription of boundary conditions, with an inflow condition only at the west face. Additionally, this enables the use of slender prismatic LES domains, which maximizes the fetch over which turbulence can develop. Therefore, the computational cost of a certain fetch is minimized [39]. The horizontal velocity field was rotated $-135.76°$, which is the averaged wind direction. Fig. 8b shows both the original and the rotated velocity vectors at different heights. Notice that the velocity vector angle varies with height.

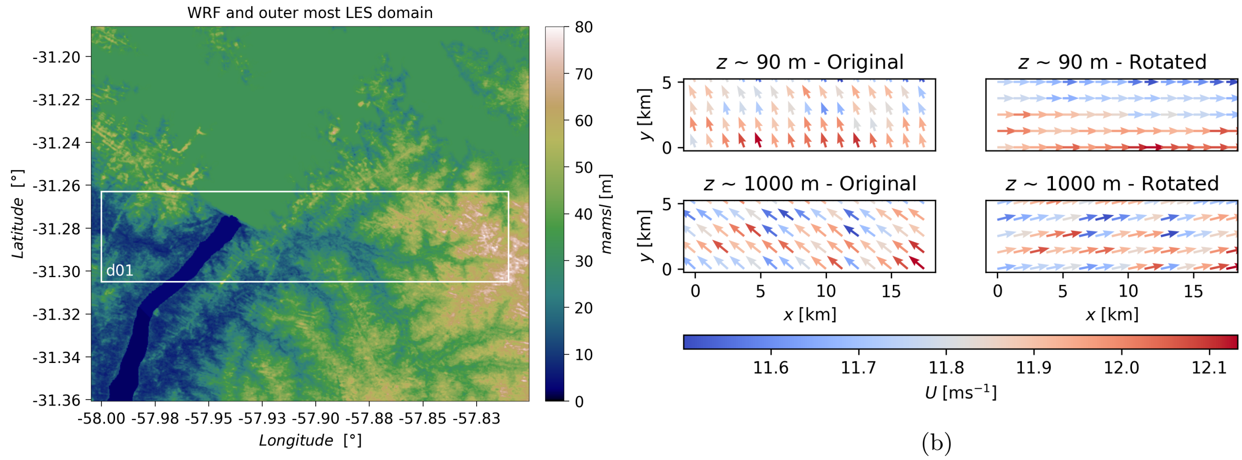

(b)

(a)

Figure 8: (a) WRF and the outermost LES domains, $d01$, disposition over ASTER-GDEM topography of the region. (b) Original and rotated horizontal velocity vectors at different heights.

Some previous works, show that nesting a finer LES domain within a coarser LES domain provides superior results regarding turbulence development and assimilation of a mesoscale model meteorological conditions [19]. Therefore, three nesting levels with successively finer horizontal resolution: 312, 100 and 20 m were implemented. The outermost domain ($d01$) receives its inflow velocity and temperature condition from interpolated fields obtained by mesoscale simulations using a WRF simulation of the same resolution as $d01$. Furthermore, the surface temperature and heat flux from WRF is prescribed to the surface of all the domains.

The two innermost domains ($d02$ and $d03$) were respectively divided in 3 and 48 computational regions that takes advantage of the Message Passage Interface (MPI) communication protocol in order to compute each region in a different CPU core. Table 1 defines the implemented domains and Fig. 9 show a schematic representation of the nested grids.

Model	Nesting level	Cells	Domain [km]	$\Delta x/\Delta y$ [m]	Δz_{min} [m]	Regions
WRF	-	$64 \times 64 \times 96$	$20 \times 20 \times 9.4$	312	-	-
caffa3d	1	$59 \times 16 \times 96$	$18.4 \times 5 \times 2$	312	1	1
caffa3d	2	$150 \times 90 \times 96$	$16.5 \times 4 \times 1.8$	100	3.3	3
caffa3d	3	$768 \times 100 \times 120$	$15.36 \times 2 \times 1.5$	20	2	48

Table 1: Simulated setup including the WRF simulation and the LES nested domains.

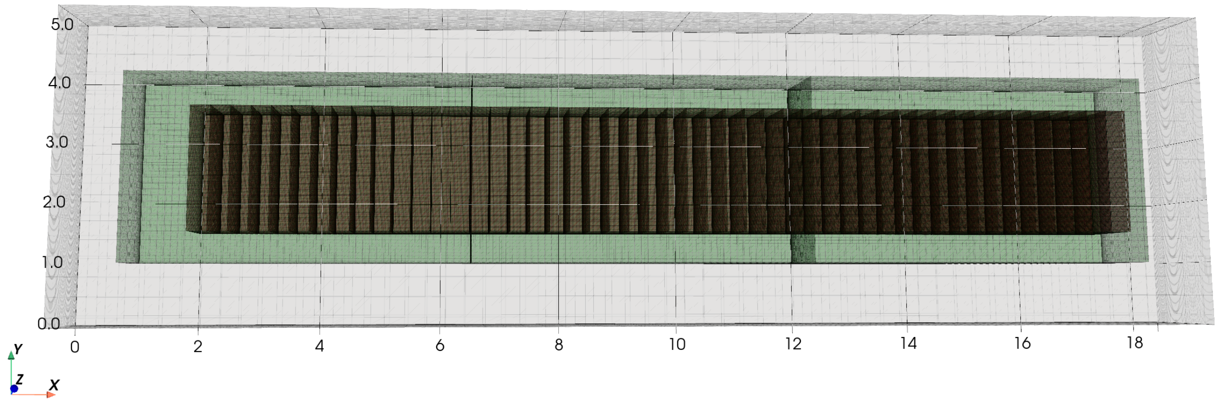

(a)

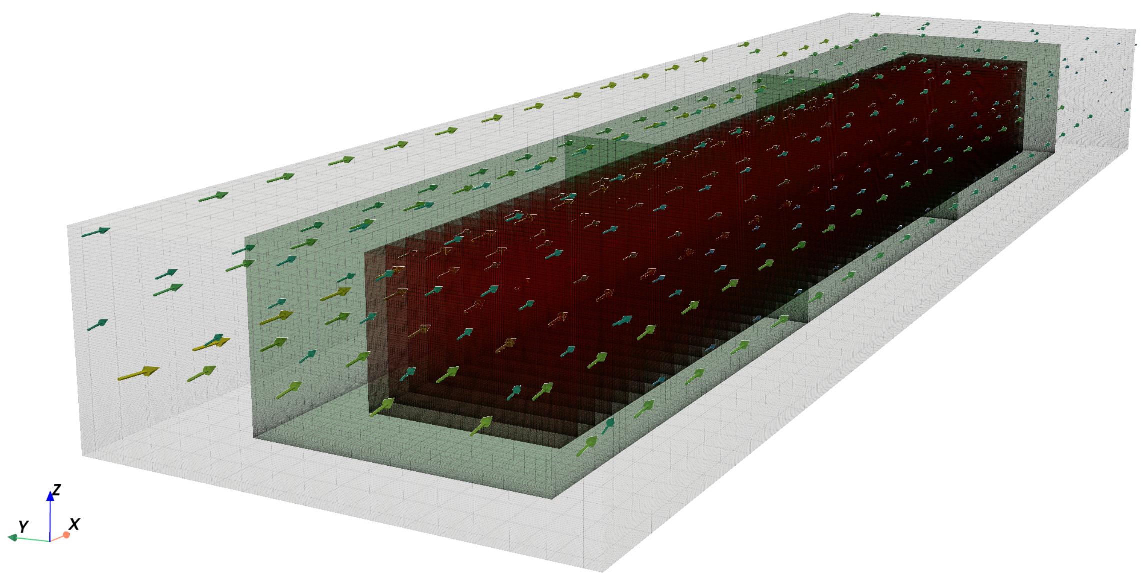

(b)

Figure 9: (a) Top 3D view of nested LES grids separated by regions. $d01$ has 1 region, $d02$ 3 regions, and $d03$ 48 regions. Units are in km. (b) Schematic view of all the grids, their regions and the velocity direction of $d01$ indicated with arrows. Dimensions and number of regions of the domains can be seen in Table 1.

Care should be taken regarding the aspect ratio of the cells near the ground when including topography into a simulation. If the cells are too stretched horizontally an interpolation between two cell centers may end up outside those cells, which could generate numerical problems. In order to solve this issue, in this work, an aspect ratio of length to height of no more than 1:30 is chosen for the cells near the ground.

Another aspect that requires attention, is that ($d01$) fall in the *terra incognita* (see Section 1) given that the coarser grid has a resolution of 300 m, and the PBL depth is about $\sim 400\,\mathrm{m}$ as appreciated in the capping inversion shown in the WRF simulation temperature profile in Fig. 5a. This brings issues related to the convective structures that develops in the nested domains.

According to previous studies [22, 40] a general rule of thumb for placing lateral boundaries in nested simulations is to extend the domains as far away from the region of interest as possible, so that flow coming from the parent domain has time and space to develop turbulent motion resolvable on the inner grid and to avoid drastic changes in terrain. Regarding the latter, as the terrain of the region study is mostly flat (Fig. 4) it is not expected to be an issue. Regarding the first point, with the computational resources at hand, the largest domains possible were implemented. Although a possible task for future work would be to extend the domains in the y axis (spanwise direction). [39] Another recommendation which was taken into account is that the parent domain on each nesting level should not be more than 3 or 4 times coarser than its child [41].

5 Results and discussion

A caffa3d-LES simulation with three nested domains of increasing resolution was performed. 52 computational regions were used. The simulation was ran for 6 h with a time step of 1 s. The simulated flow becomes stationed at about 2 h. Following Mazzaro [1], the last three simulation hours were used to calculate mean fields. In Fig. 10 the time evolution of all instantaneous horizontal velocity components for different heights in $d03$ at 16.9 km from the inflow is shown. Notice how at $z \sim 1000\,\mathrm{m}$ the velocity is much less dispersed because the turbulent motion ceased to exist above the PBL height. The PBL depth or height is determined by the base of the capping inversion [2] and as shown in Fig. 5 and Fig.12b this is around $\sim 400\,\mathrm{m}$.

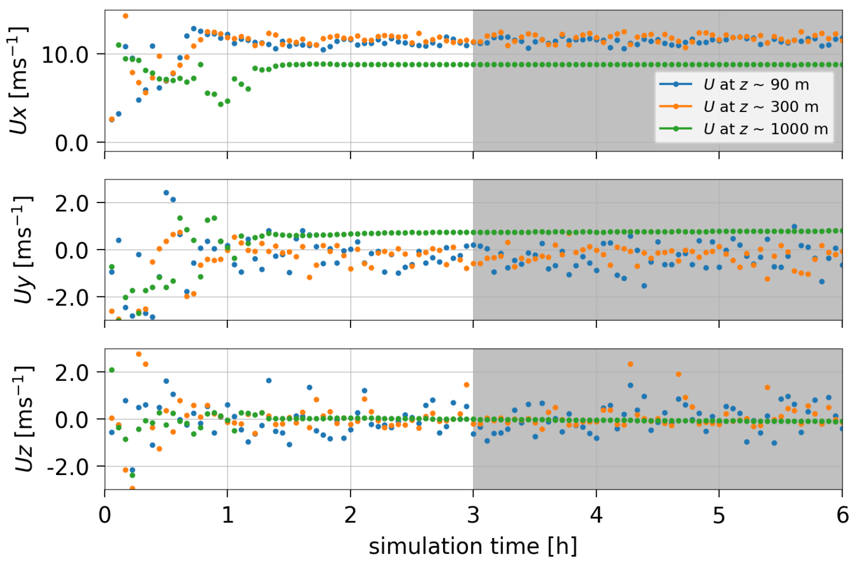

Figure 10: Time evolution of instantaneous velocity components at $z \sim 90$, 300 and 1000 m. The shaded gray area represents the time interval used for the analysis of the simulations (3 to 6 h). Velocity was sampled in $d03$ at $x \sim 16.9\,\mathrm{km}$

The successively finer nested grids domains prove to be a successful strategy to generate turbulence while assimilating the mean mesoscale flows. This is in accordance with the results presented in [1, 3, 9, 19]. Fig. 11 depicts a spanwise view of the vertical velocity component instantaneous field, with the three levels of nesting (312, 100 and 20 m of horizontal resolution) overlapped. The convective structures are fully developed in the inner most domain $d03$, partially developed in $d02$, and almost with no development in $d01$. This slice was taken at 16 km from the inflow as indicated in the lower subplot that shows a top view of the nested grid. Furthermore, it can be qualitative appreciated that the PBL height marks a clear constraint to the turbulent motion which is consistent with the prescribed mesoscale temperature profile (see Fig. 5 and Fig. 6).

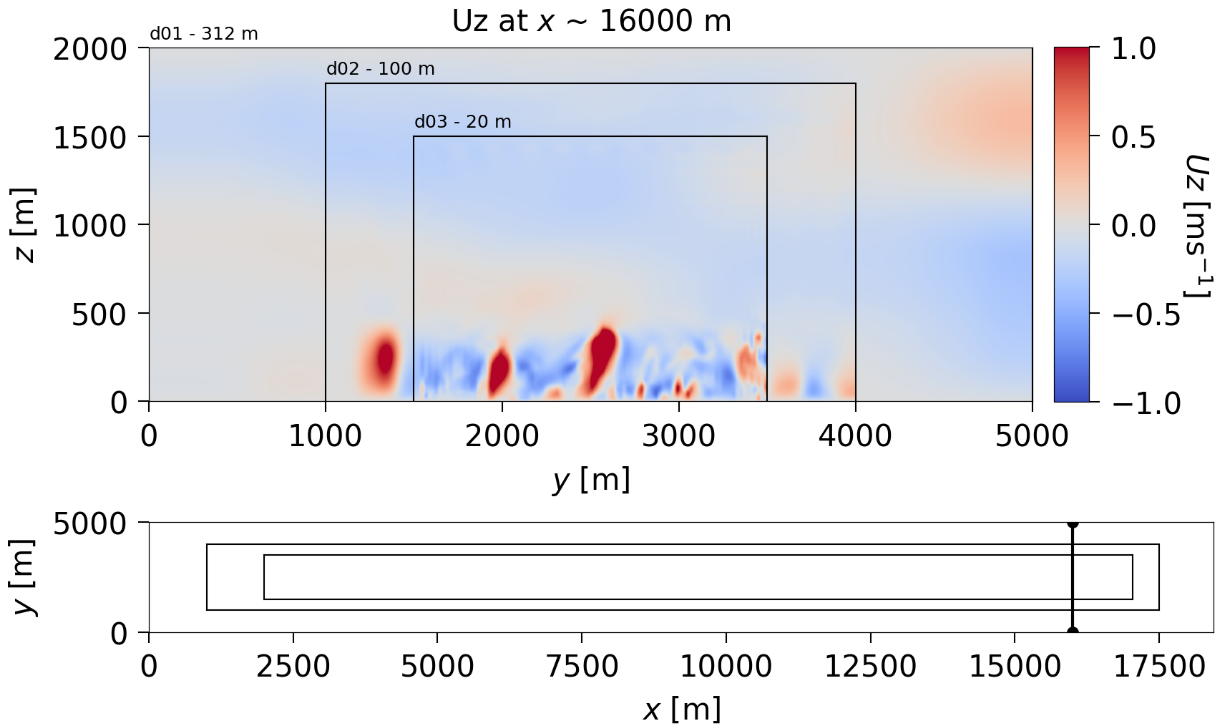

(a)

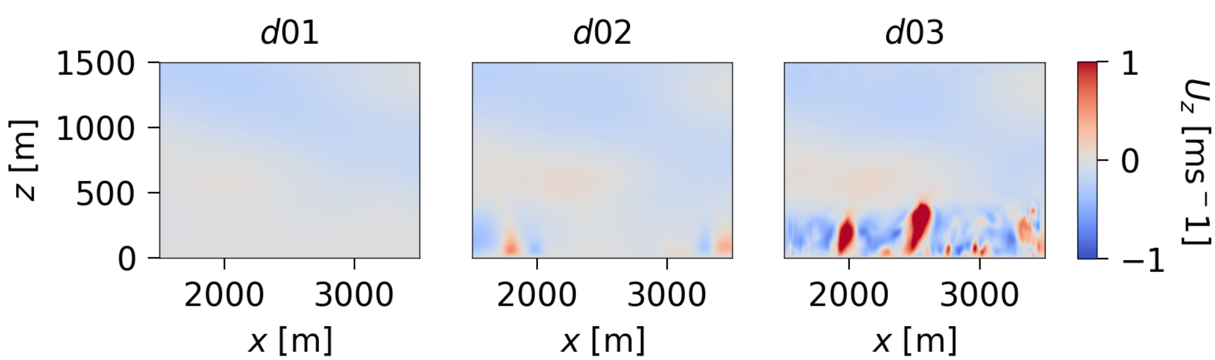

(b)

Figure 11: Spanwise view of instantaneous vertical velocity component (Uz) after 6 h of simulation of the three nested domains (a) overlapped and (b) separated in different subplots and sliced to have $d03$ dimensions.

The mean fields of all the domains are consistent with the mesoscale fields, as can be appreciated in Fig. 12. This proves that the overlapping nesting technique is useful to pass the mean flow to the nested domains and that the mesoscale flow passed as inflow boundary condition is well assimilated by the finer LES domains. However, given that the Uy profile presents some departure from the mesoscale flow some other consideration should be taken in order to handle this problem. Besides, the capping inversion seems to be more diluted in the LES domains; further studies are needed to assess this issue.

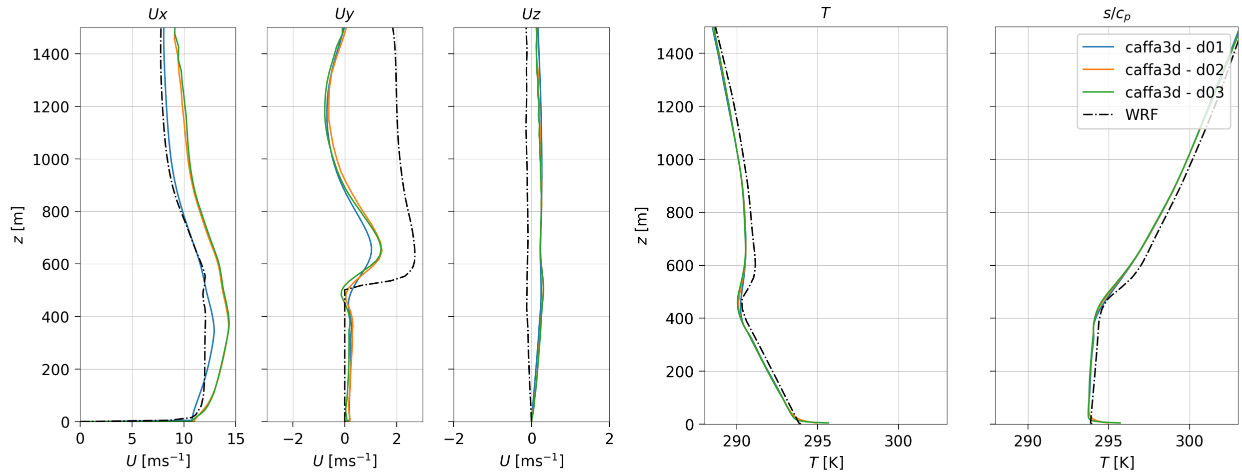

(a) (b)

Figure 12: (a) Mean velocity profiles of WRF and all three caffa3d-LES simulations. (b) Absolute temperature and dry static energy profiles for WRF and caffa3d-LES simulations. Mean taken between 3 and 6 h of simulation (See Fig. 10). Profiles taken at 16 km from the inflow along the centerline of the domain.

Fig. 13a shows temporally averaged velocity profiles in $d03$. Each line corresponds to a different position along the x axis. The dotted-dashed black line corresponds to the WRF simulation profile at the inflow of $d01$, as $d03$ inherits the flow conditions from $d01$. A lack of consistency between the mesoscale and the LES solutions for Uy can be noticed. This may be caused by the shape of the domains, which may be too narrow with respect to the y direction, considering that the prevailing inflow direction is not exactly aligned with the x axis at every height (see Fig. 8b).

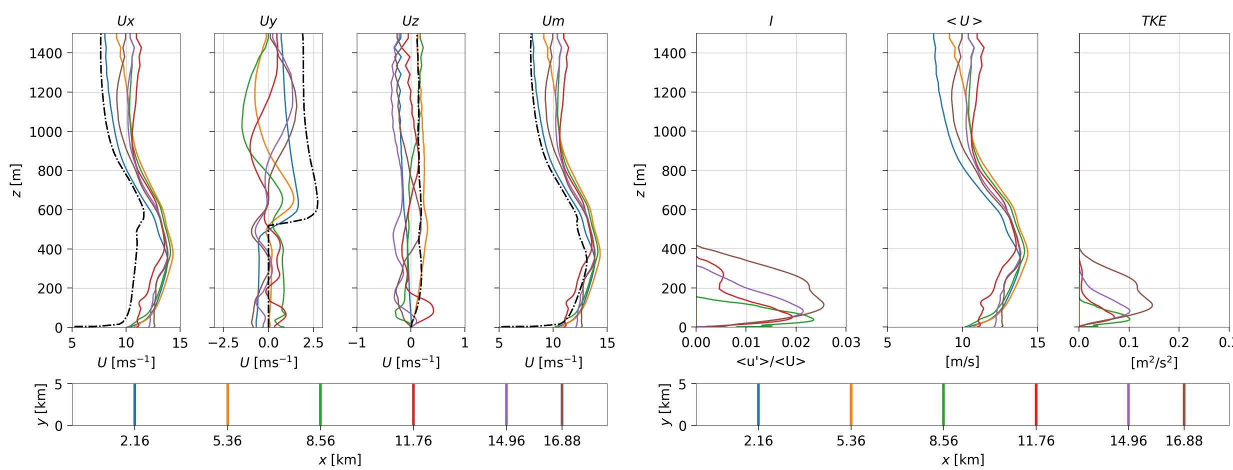

(a) (b)

Figure 13: (a) Vertical profiles for all velocity components and the velocity module for $d03$ domain. The black dotted-dashed line represents the profile of the WRF simulation at the inflow of $d01$. (b) From left to right: Turbulence Intensity (I), mean velocity module ($< U >$) and Turbulent Kinetic Energy (TKE). All magnitudes are averaged over a 3 h window (see Fig. 10) and taken in the spanwise center of the domain, except for I and TKE which are averaged along the y axis.

The presence of convective structures in $d03$, namely thermals, can be deduced from Fig. 14. This eddies move upwards and downwards transporting mass and heat and are responsible for the mixing of the PBL.

These structures are elongated along the x axis (right of Fig. 14) following the flow stream, and so they are narrow in the spanwise direction (bottom left of Fig. 14). Their height is the PBL depth (both bottom and top left of Fig. 14). They ascend up to heights determined by the θ profile which are around 400 m as was commented previously. The *TKE* contours (Fig. 16) are also consistent with this observation.

Additionally, Fig. 15 depicts a horizontal and streamwise view of instantaneous contours of Ux and Uz where the convective eddies can be appreciated.

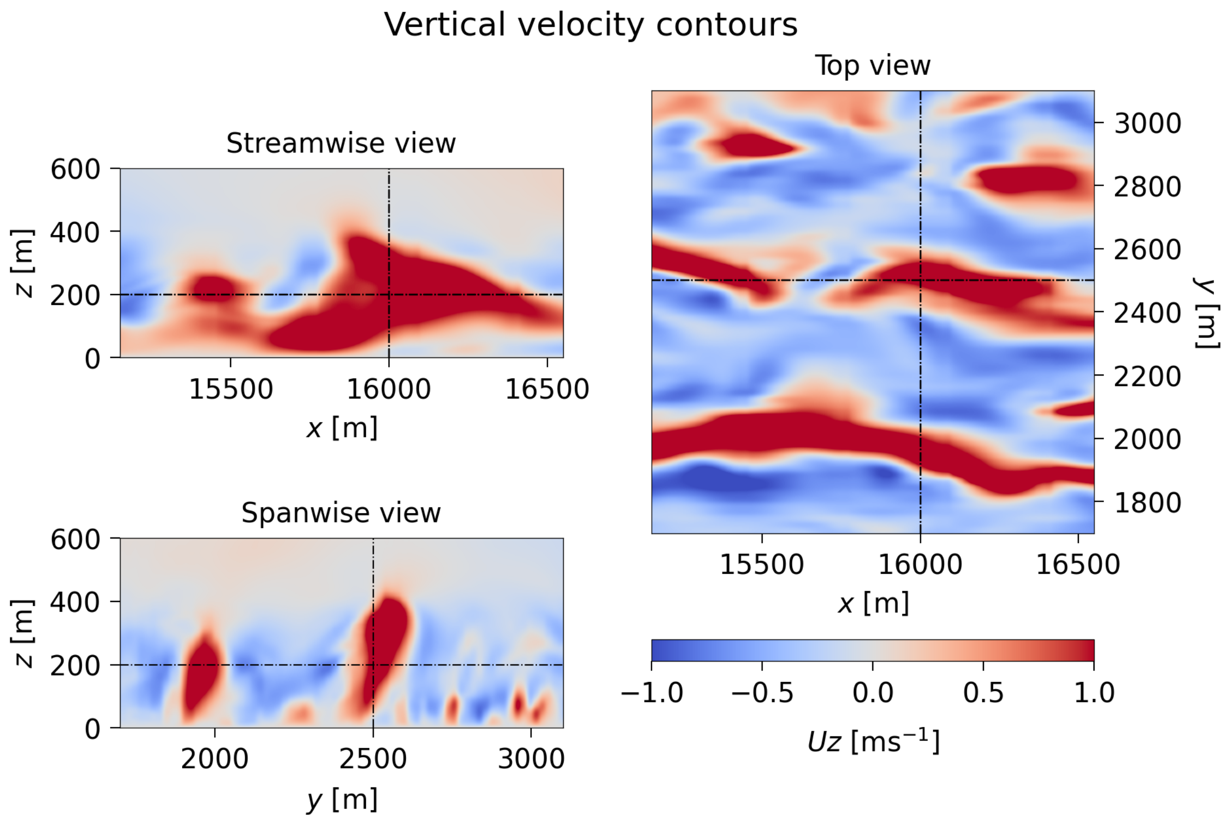

Figure 14: Contours of vertical velocity in the streamwise, spanwise direction and top view (at $z \sim 200\,\mathrm{m}$) as described in each subplot title. The slices are taken to appreciate the convective structures, or thermals that form in the PBL. The dotted-dashed lines indicate the position of each one of the other subplots.

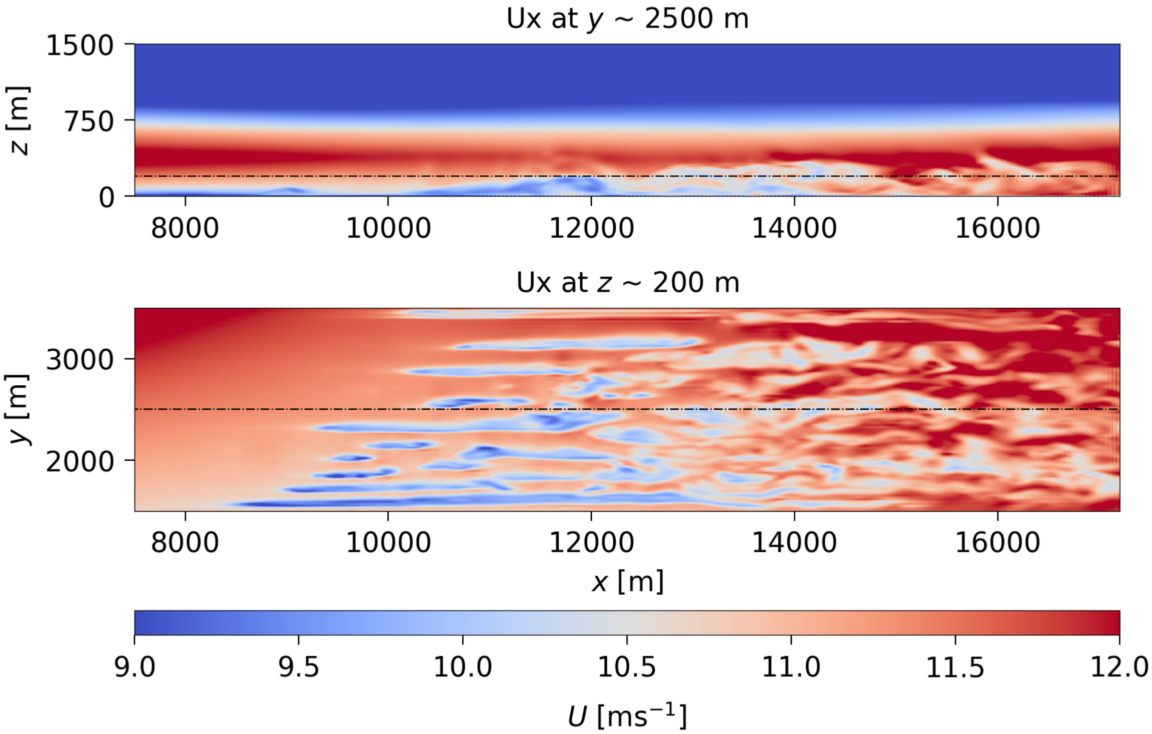

(a)

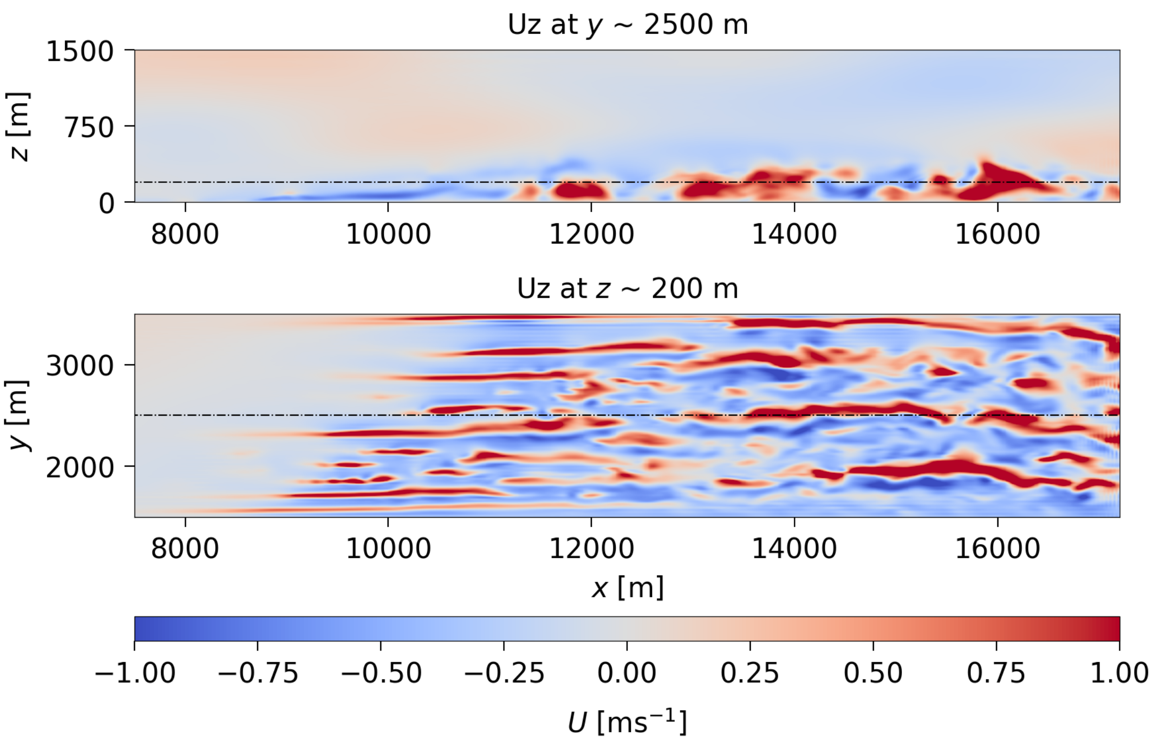

(b)

Figure 15: Streamwise (top) and horizontal (bottom) views of contours of instantaneous (a) horizontal velocity component Ux and (b) vertical velocity component Uz in $d03$ after 6 h of simulation.

Comparing the total mesoscale *TKE* (Fig. 6) (which is parametrized and not resolved as it is a RANS model [10]) with the resolved one in the finer grid LES domain (Fig. 16) a good consistency is observed. Nonetheless, the comparison can only be qualitative, and a comparison of other metrics are needed.

Larger domains are needed for a full stabilization of the *TKE* field, as shown in the bottom suplot of Fig. 16. This is in line with state of the art works on the matter like Mazzaro [1].

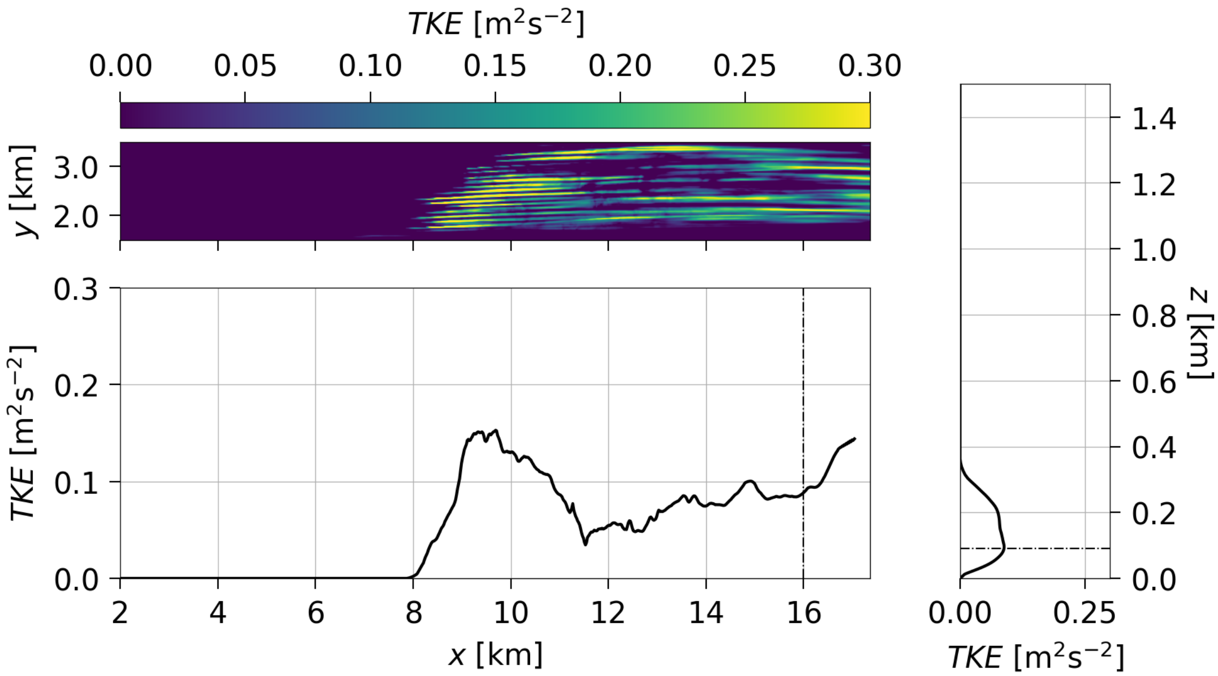

Figure 16: At the top left, caffa3d $d03$ simulation resolved *TKE* field at $z \sim 90\,\text{m}$. *TKE* evolution over fetch at the bottom left, and *TKE* vertical profile at $x \sim 16\,\text{km}$ at the right. In all subplots (except in the contour), *TKE* was temporally averaged in a 3 h window (see Fig. 10) and spacially in the spanwise y axis.

6 Conclusions

An offline one-way coupling technique with the mesoscale model WRF and the in-house LES model caffa3d was implemented in combination with high-resolution nested LES simulations in order to model a convective PBL. Simulations were performed over real terrain with realistic initial and inflow boundary conditions from the mesoscale model in a morning that exhibits a convective PBL with its characteristic capping inversion.

Preliminar results show that mesoscale flow is successfully assimilated into caffa3d-LES domains as shown in Fig. 12. Some additional tests may be necessary to optimize the LES grids in order to improve the discrepancies found between WRF and LES results regarding the spanwise velocity, as shown in Fig. 13a. Two causes may explain this issue: the rotation of the wind field (as it results in a unrealistic profile of Uy) and the narrowness of the LES grids. The latter is a consideration well documented in the literature [1, 3, 9, 39, 42] that could not be considered in time for computational resources reasons.

Although the rotation of the horizontal velocity fields proved to be an efficient way to have satisfactory results without the need for huge domains, given that the topography was not rotated, either a rotation of the LES grids respective to the real terrain and prevailing wind direction or larger domains without any rotation is needed for a realistic account of the flow in the site.

Turbulent motion is successfully developed in the innermost domain. It is noteworthy that the incorporation of the third nesting level while maintaining a relative large fetch were key factors to accomplish this. The need for a finer LES grid of about 20 m in horizontal resolution for convective structures to be fully resolved is consistent with other work in the matter [23]. As mentioned, a considerably large fetch of at least 12 km was required in order to reach a somewhat stable *TKE*, though longer fetches are needed for the *TKE* to fully stabilize.

Convective structures were observed and examined and are consistent with the characteristics of a CBL as accounted in many works. [1, 2, 9, 19]

Overall, the technique proves to be a good approach to bridge the mesoscale and the microscale. These results encourage a continuation of the work to attend some of the issues encountered here. Some of that work is briefly summarized in the following section.

7 Future work

One of the main conclusions of this work is that in order to overcome the issue of the *terra incognita* partially resolved convective structures is to have long enough fetches of about 40 km that enable a full stabilization of turbulence and ensures a realistic value of first-order quantities (θ and U), and resolved turbulent statistics like *TKE* [1]. As stated in the previous sections, wider domains may be necessary for a correct assimilation of the horizontal spanwise component Uy as suggested in previous works [1, 42].

On balance, larger domains of ideally 50×50 km may be needed to avoid any issue with the stabilization of turbulent motions and with the prevailing wind direction.

The coupling and nesting technique implemented in this work is pending validation. For instance, field measurements could be taken and compare them to the presented results. Besides, a sensitivity study to three key model aspects should be performed: grid resolution, turbulence closure and placement of the nested domains [22].

Following related work in the field, it could be useful to apply a perturbation method, like the Stochastic Perturbation Method (applied to the potential temperature field for instance) in order to stimulate the onset of turbulent motion and decrease the fetch [1, 3, 9, 39, 43, 44].

Other consideration may be necessary given that the low depth of the PBL makes the coarser grids to enter the *terra incognita*. Some techniques have been proposed for modeling this situation, such as scale-aware parametrizations, and quasi-3D multi-scale techniques [45].

It would be preferable to use a Raleigh damping layer over the upper 400 m of the domain to damp oscillations and to force the free tropospheric temperature and wind fields toward specified values, the latter representing the geostrophic wind used to force the mean flow [39].

The prescription of the mesoscale simulation humidity field to caffa3d together with the implementation of a module that contemplates the physics of humid air would enable to model all atmosphere physics phenomena, including the original motivation of this work that was to accurately model PBL clouds (stratocumulus) [38].

In the case study presented in this work, given the described low atmosphere characteristics, the mostly flat terrain, the time of the day, and the temperature profile, the PBL it is assumed to be buoyancy-driven. However, a more demonstration of that would be to analyze the *TKE* budget (for instance, see Moeng [46]) in order to clearly identify the PBL regime.

In relation to this, a WRF simulation of other day with a clearer capping inversion and with stronger and deeper PBL (perhaps in the afternoon) would be good to test this technique with a more paradigmatic CBL.

Last but not least, in order to accelerate the computational time of these simulation (thus enabling to simulate larger domains) an implementation of this coupling technique and this case setup can be performed using heterogeneous computing parallelization techniques with GPU computing hardware and CUDA. Some work has already been done using a CUDA implementation of caffa3d flow solver. [47, 48]

8 Acknowledgments

This work are partial results of my Master's thesis that was possible thanks to the financial support of the National Agency for Research and Innovation (ANII) of Uruguay. What is more, ANII also financed the project NEFELE: *predicción de Nubes para la generación de Energía Fotovoltaica Ensamblando modelación LES y de mEsoescala* (*NEFELE: cloud prediction for photovoltaic energy ensambling LES and mesoscale modelling*) that allowed the development of the work presented in this paper.

References

[1] Laura J Mazzaro, Domingo Muñoz-Esparza, Julie K Lundquist, and Rodman R Linn. Nested mesoscale-to-LES modeling of the atmospheric boundary layer in the presence of under-resolved convective structures. *Journal of Advances in Modeling Earth Systems*, 9(4):1795–1810, 2017.

[2] Roland B Stull. *An introduction to boundary layer meteorology*, volume 13. Springer Science & Business Media, 1988.

[3] Domingo Muñoz-Esparza, Julie K Lundquist, Jeremy A Sauer, Branko Kosović, and Rodman R Linn. Coupled mesoscale-LES modeling of a diurnal cycle during the CWEX-13 field campaign: From weather to boundary-layer eddies. *Journal of Advances in Modeling Earth Systems*, 9(3):1572–1594, 2017.

[4] GC Cuchiara and B Rappenglück. Performance analysis of WRF and LES in describing the evolution and structure of the planetary boundary layer. *Environmental Fluid Mechanics*, 18(5):1257–1273, 2018.

[5] James W Deardorff. Numerical investigation of neutral and unstable planetary boundary layers. *Journal of Atmospheric Sciences*, 29(1):91–115, 1972.

[6] James W Deardorff. James W. Deardorff. *Boundary-Layer Meteorol*, 157:343–344, 2015.

[7] Domingo Muñoz-Esparza, Branko Kosović, Jeff Mirocha, and Jeroen van Beeck. Bridging the transition from mesoscale to microscale turbulence in numerical weather prediction models. *Boundary-layer meteorology*, 153(3):409–440, 2014.

[8] Bowen Zhou and Fotini Katopodes Chow. Nighttime turbulent events in a steep valley: A nested large-eddy simulation study. *Journal of the Atmospheric Sciences*, 70(10):3262–3276, 2013.

[9] Sue Ellen Haupt, Branko Kosovic, William Shaw, Larry K Berg, Matthew Churchfield, Joel Cline, Caroline Draxl, Brandon Ennis, Eunmo Koo, Rao Kotamarthi, et al. On bridging a modeling scale gap: Mesoscale to microscale coupling for wind energy. *Bulletin of the American Meteorological Society*, 100(12):2533–2550, 2019.

[10] William C Skamarock, Joseph B Klemp, Jimy Dudhia, David O Gill, Zhiquan Liu, Judith Berner, Wei Wang, Jordan G Powers, Michael G Duda, Dale M Barker, et al. A description of the advanced research WRF model version 4. *National Center for Atmospheric Research: Boulder, CO, USA*, 145:145, 2019.

[11] Yubao Liu, Tom Warner, Yuewei Liu, Claire Vincent, Wanli Wu, Bill Mahoney, Scott Swerdlin, Keith Parks, and Jennifer Boehnert. Simultaneous nested modeling from the synoptic scale to the LES scale for wind energy applications. *Journal of Wind Engineering and Industrial Aerodynamics*, 99(4):308–319, 2011.

[12] Charles Talbot, Elie Bou-Zeid, and Jim Smith. Nested mesoscale large-eddy simulations with WRF: Performance in real test cases. *Journal of Hydrometeorology*, 13(5):1421–1441, 2012.

[13] Xia Chu, Lulin Xue, Bart Geerts, Roy Rasmussen, and Daniel Breed. A case study of radar observations and WRF LES simulations of the impact of ground-based glaciogenic seeding on orographic clouds and precipitation. Part I: Observations and model validations. *Journal of applied meteorology and climatology*, 53(10):2264–2286, 2014.

[14] Raphaël Cécé, Didier Bernard, Jérôme Brioude, and Narcisse Zahibo. Microscale anthropogenic pollution modelling in a small tropical island during weak trade winds: Lagrangian particle dispersion simulations using real nested LES meteorological fields. *Atmospheric environment*, 139:98–112, 2016.

[15] Raj K Rai, Larry K Berg, Branko Kosović, Jeffrey D Mirocha, Mikhail S Pekour, and William J Shaw. Comparison of measured and numerically simulated turbulence statistics in a convective boundary layer over complex terrain. *Boundary-Layer Meteorology*, 163(1):69–89, 2017.

[16] Andrzej A Wyszogrodzki, Shiguang Miao, and Fei Chen. Evaluation of the coupling between mesoscale-WRF and LES-EULAG models for simulating fine-scale urban dispersion. *Atmospheric Research*, 118:324–345, 2012.

[17] Guixing Chen, Xinyue Zhu, Weiming Sha, Toshiki Iwasaki, Hiromu Seko, Kazuo Saito, Hironori Iwai, and Shoken Ishii. Toward improved forecasts of sea-breeze horizontal convective rolls at super high resolutions. Part I: Configuration and verification of a Down-Scaling Simulation System (DS3). *Monthly Weather Review*, 143(5):1849–1872, 2015.

[18] D Muñoz-Esparza, B Kosović, J Van Beeck, and J Mirocha. A stochastic perturbation method to generate inflow turbulence in large-eddy simulation models: Application to neutrally stratified atmospheric boundary layers. *Physics of Fluids*, 27(3):035102, 2015.

[19] Jeff Mirocha, Branko Kosović, and Gokhan Kirkil. Resolved turbulence characteristics in large-eddy simulations nested within mesoscale simulations using the Weather Research and Forecasting Model. *Monthly Weather Review*, 142(2):806–831, 2014.

[20] Paul M Markowski and George H Bryan. LES of laminar flow in the PBL: A potential problem for convective storm simulations. *Monthly Weather Review*, 144(5):1841–1850, 2016.

[21] John C Wyngaard. Toward numerical modeling in the "Terra Incognita". *Journal of the atmospheric sciences*, 61(14):1816–1826, 2004.

[22] Bowen Zhou and Fotini Katopodes Chow. Nested large-eddy simulations of the intermittently turbulent stable atmospheric boundary layer over real terrain. *Journal of the Atmospheric Sciences*, 71(3):1021–1039, 2014.

[23] Bowen Zhou, Jason S Simon, and Fotini K Chow. The convective boundary layer in the terra incognita. *Journal of the Atmospheric Sciences*, 71(7):2545–2563, 2014.

[24] J Ching, R Rotunno, M LeMone, A Martilli, B Kosovic, PA Jimenez, and J Dudhia. Convectively induced secondary circulations in fine-grid mesoscale numerical weather prediction models. *Monthly Weather Review*, 142(9):3284–3302, 2014.

[25] G Usera, ANTON Vernet, and JA Ferré. A parallel block-structured finite volume method for flows in complex geometry with sliding interfaces. *Flow, Turbulence and Combustion*, 81(3):471–495, 2008.

[26] Mariana Mendina, Martin Draper, Gabriel Narancio, Gabriel Usera, and Ana Paula Kelm Soares. A General Purpose Parallel Block Structured Open Source Flow Solver. In *2012 Seventh International Conference on P2P, Parallel, Grid, Cloud and Internet Computing, pages=273–278, year=2012, organization=IEEE*.

[27] Mariana Mendina, Martin Draper, Ana Paula Kelm Soares, Gabriel Narancio, and Gabriel Usera. A general purpose parallel block structured open source incompressible flow solver. *Cluster Computing*, 17(2):231–241, 2014.

[28] Joseph Smagorinsky. General circulation experiments with the primitive equations: I. The basic experiment. *Monthly weather review*, 91(3):99–164, 1963.

[29] Daniel Freire. Implementación computacional de la interacción sólido-fluido para el modelo caffa3d.mbri. *FI. Tesis de Doctorado. ISSN 1688-2776*, 2018.

[30] Hidajet Hadzic. *Development and application of finite volume method for the computation of flows around moving bodies on unstructured, overlapping grids*. Technische Universität Hamburg, 2006.

[31] Akio Arakawa and Vivian R Lamb. Computational design of the basic dynamical processes of the UCLA general circulation model. *General circulation models of the atmosphere*, 17(Supplement C):173–265, 1977.

[32] AS Monin. Basic turbulent mixing laws in the atmospheric surface layer. *Tr. Akad. Nauk SSSR Geofiz. Inst*, 24:163–187, 1954.

[33] Tetsushi Tachikawa, Masami Hato, Manabu Kaku, and Akira Iwasaki. Characteristics of ASTER GDEM version 2. In *2011 IEEE international geoscience and remote sensing symposium, pages=3657–3660, year=2011, organization=IEEE.*

[34] Russ Rew and Glenn Davis. NetCDF: an interface for scientific data access. *IEEE computer graphics and applications*, 10(4):76–82, 1990.

[35] Song-You Hong, Yign Noh, and Jimy Dudhia. A new vertical diffusion package with an explicit treatment of entrainment processes. *Monthly weather review*, 134(9):2318–2341, 2006.

[36] Song-You Hong. A new stable boundary-layer mixing scheme and its impact on the simulated East Asian summer monsoon. *Quarterly Journal of the Royal Meteorological Society*, 136(651):1481–1496, 2010.

[37] Xiao-Ming Hu, Petra M Klein, and Ming Xue. Evaluation of the updated YSU planetary boundary layer scheme within WRF for wind resource and air quality assessments. *Journal of Geophysical Research: Atmospheres*, 118(18):10–490, 2013.

[38] Robert Wood. Stratocumulus clouds. *Monthly Weather Review*, 140(8):2373–2423, 2012.

[39] SE Haupt, Larry K Berg, A Decastro, David J Gagne, Pedro Jimenez, Timothy Juliano, Branko Kosovic, Jeff D Mirocha, Eliot Quon, Jeremy Sauer, et al. Report of the Atmosphere to Electrons Mesoscale-to-Microscale Coupling Project (FY2019). Technical report, Pacific Northwest National Lab.(PNNL), Richland, WA (United States . . . , 2019.

[40] Bowen Zhou and Fotini Katopodes Chow. Large-eddy simulation of the stable boundary layer with explicit filtering and reconstruction turbulence modeling. *Journal of the Atmospheric Sciences*, 68(9):2142–2155, 2011.

[41] Ping Zhu, Bruce A Albrecht, Virendra P Ghate, and Zhenduo Zhu. Multiple-scale simulations of stratocumulus clouds. *Journal of Geophysical Research: Atmospheres*, 115(D23), 2010.

[42] CH Moeng, Jimy Dudhia, Joe Klemp, and Peter Sullivan. Examining two-way grid nesting for large eddy simulation of the PBL using the WRF model. *Monthly weather review*, 135(6):2295–2311, 2007.

[43] Domingo Muñoz-Esparza and Branko Kosović. Generation of inflow turbulence in large-eddy simulations of nonneutral atmospheric boundary layers with the cell perturbation method. *Monthly Weather Review*, 146(6):1889–1909, 2018.

[44] LJ Mazzaro, E Koo, D Muñoz-Esparza, JK Lundquist, and RR Linn. Random force perturbations: A new extension of the cell perturbation method for turbulence generation in multiscale atmospheric boundary layer simulations. *Journal of Advances in Modeling Earth Systems*, 11(7):2311–2329, 2019.

[45] A Arakawa, J-H Jung, and C-M Wu. Toward unification of the multiscale modeling of the atmosphere. *Atmospheric Chemistry and Physics*, 11(8):3731–3742, 2011.

[46] Chin-Hoh Moeng and Peter P Sullivan. A comparison of shear-and buoyancy-driven planetary boundary layer flows. *Journal of Atmospheric Sciences*, 51(7):999–1022, 1994.

[47] B López, A Guggeri, M Draper, and G Usera. Assessment of a heterogeneous computing CFD code in wind farm simulations. In *Journal of Physics: Conference Series, volume=2265, number=4, pages=042046, year=2022, organization=IOP Publishing.*

[48] Gonzalo Fernandez, Mariana Mendina, and Gabriel Usera. Heterogeneous Computing (CPU–GPU) for pollution dispersion in an urban environment. *Computation*, 8(1):3, 2020.